JNK inhibition enhances cell–cell adhesion impaired by desmoglein 3 gene disruption in keratinocytes

Shuhei Ogawa[1], Takashi Ishii[2], Takahito Otani[3], Yuko Inai[4], Takashi Matsuura[1], Tetsuichiro Inai*[, 3, 5]

[1]Department of Oral Rehabilitation, Fukuoka Dental College, 2-15-1 Tamura, Sawara-ku, Fukuoka 814-0193, Japan

[2]Department of Nutrition and Dietetics, School of Family and Consumer Sciences, Kamakura Women's University, Kanagawa 247-0056, Japan

[3]Department of Morphological Biology, Fukuoka Dental College, 2-15-1 Tamura, Sawara-ku, Fukuoka 814-0193, Japan

[4]Division of General Dentistry, Kyushu University Hospital, 3-1-1 Maidashi, Higashi-ku, Fukuoka 812-8582, Japan

[5]Oral Medicine Research Center, Fukuoka Dental College, 2-15-1 Tamura, Sawara-ku, Fukuoka 814-0193, Japan

***Corresponding author:** Tetsuichiro Inai, D.D.S., Ph.D., Department of Morphological Biology, Fukuoka Dental College, 2-15-1 Tamura, Sawara-ku, Fukuoka 814-0193, Japan

Tel: +81-92-801-0411 Ext. 683, Fax: +81-92-801-4909

E-mail address: tinaitj@fdcnet.ac.jp, ORCID: 0000-0002-3684-960X

Acknowledgements The authors would like to thank Editage for English proofreading.

Funding This study was supported in part by a Grant-in-Aid for Scientific Research (C) (No. 22K09921) from the Ministry of Education, Culture, Sports, Science, and Technology in Japan.

Abstract

c-Jun NH_2-terminal protein kinase (JNK) and p38 are stress-activated mitogen-activated protein kinases (MAPK) that are phosphorylated by various stimuli. It has been reported that the loss of desmoglein (DSG) 3, a desmosomal transmembrane core molecule, in keratinocytes impairs cell–cell adhesion accompanied by p38 MAPK activation. To understand the biological role of DSG3 in desmosomes and its relationship with stress-activated MAPKs, we established DSG3 knockout keratinocytes (KO cells). Wild-type cells showed a linear localization of DSG1 to cell–cell contacts, whereas KO cells showed a remarkable reduction despite the increased protein levels of DSG1. Cell–cell adhesion in KO cells was impaired over time, as demonstrated by dispase-based dissociation assays. The linear localization of DSG1 to cell–cell contacts and the strength of cell–cell adhesion were promoted by the pharmacological inhibition of JNK. Conversely, pharmacological activation of JNK, but not p38 MAPK, in wild-type cells reduced the linear localization of DSG1 in cell–cell contacts. Our data indicate that DSG1 and DSG2 in KO cells cannot compensate for the attenuation of cell–cell adhesion strength caused by DSG3 deficiency and that JNK inhibition restores the strength of cell–cell adhesion by increasing the linear localization of DSG1 in cell–cell contacts in KO cells. Inhibition of JNK signaling may

improve cell–cell adhesion in diseases in which DSG3 expression is impaired.

Keywords: keratinocyte; desmosome; desmoglein; mitogen-activated protein kinase

Introduction

Cell–cell adhesion derived from adherens junctions and desmosomes maintains the structural integrity of epithelial tissues. Adherens junctions are formed by classical cadherins, including E- and P-cadherins, which are linked to the actin cytoskeleton by catenins (Garcia et al. 2018). The establishment of adherens junctions is a prerequisite for desmosome and tight junction formation (Watabe et al. 1994). Desmosomes, which resist mechanical stress, are composed of desmosomal cadherins, desmogleins (DSGs) 1–4, and desmocollins (DSCs) 1–3, which are linked to keratin intermediate filaments via plakoglobin and desmoplakin (Delva et al. 2009; Garrod and Chidgey 2008). Cadherins are Ca^{2+}-dependent cell adhesion molecules that form the cadherin superfamily to which DSGs and DSCs belong.

Pemphigus is a life-threatening autoimmune blistering disease of the skin and mucous membranes. Patients have autoantibodies against DSG1 and DSG3, resulting in the loss of cell–cell adhesion (acantholysis). DSG1 and DSG3 are the principal pemphigus antigens of pemphigus foliaceus (PF) and pemphigus vulgaris (PV), respectively (Amagai and Stanley 2012; Stanley and Amagai 2006). Blisters principally occur in the oral mucous membrane in patients with PV at an early stage, and within the granular layers of the superficial epidermis in patients with PF. As the disease progresses in patients with PV, blisters occur deep in the epidermis

between the basal and most immediate suprabasal keratinocytes, as well as the basal cells themselves. The distribution and expression levels of DSG1 and DSG3 may account for the characteristic distribution of lesions caused by autoantibodies in patients with PF and PV, which reduce the DSG1- and DSG3-mediated intercellular adhesion of keratinocytes by steric hindrance (Mahoney et al. 1999; Shirakata et al. 1998; Stanley and Amagai 2006; Waschke and Spindler 2014).

Mitogen-activated protein kinases (MAPKs) are a family of serine-threonine kinases involved in the modulation of cellular responses (Bogoyevitch and Court 2004; Hagemann and Blank 2001; Pearson et al. 2001; Schaeffer and Weber 1999). MAPKs include extracellular signal-regulated kinase-1 and -2 (ERK1/2), c-Jun NH_2-terminal kinases (JNK1/2/3), p38 (p38α/β/γ/δ) MAPK, ERK3/4, ERK5, and ERK7/8 in mammalian cells (Kyriakis and Avruch 2001). JNK and p38 are stress-activated MAPKs that are phosphorylated by various stimuli. Keratinocytes in the oral mucosal epithelium are exposed to various stimuli from the surface, including mechanical, thermal, pH, and osmotic stresses. Although steric hindrance by autoantibodies against DSG1 and/or DSG3 in patients with pemphigus may be considered pathogenic, the involvement of the p38 MAPK signaling pathway in PV pathogenesis was first shown in keratinocytes treated with PV Immunoglobulin G (IgG) (Berkowitz et al. 2005). p38 MAPK inhibition in a mouse model of PV prevented blister formation (Berkowitz et al. 2006). JNK and p38 MAPK are involved in the assembly and disassembly of tight junctions in keratinocytes (Minakami et al. 2015; Siljamäki et al. 2014) and other cells (Kojima et al. 2010; Naydenov et al. 2009). The inhibition of JNK by SP600125 induces tight junction formation in HaCaT cells (Aono and Hirai 2008; Kitagawa et al. 2014). However, whether JNK is involved in desmosome assembly and disassembly in

keratinocytes has not yet been investigated.

To investigate whether disruption of DSG3 in keratinocytes affects desmosomes, we established DSG3 gene-disrupted K38 cells (a mouse keratinocyte cell line). Although primary human epidermal keratinocytes are commercially available, they have limited proliferation and are not suitable for establishing DSG3 gene-disrupted cells. Because we established three-dimensional cultures to form keratinized and non-keratinized stratified epithelia using K38 cells (Nikaido et al. 2019; Ishikawa et al. 2022), we can investigate the biological role of DSG3 in two- and three-dimensional cultures. Therefore, we used K38 cells to disrupt the DSG3 gene. We found that the loss of DSG3 impaired cell–cell adhesion and concomitantly reduced the linear localization of DSG1 in cell–cell contacts. Inhibition of JNK, compared to that of p38 MAPK, more effectively restored impaired cell–cell adhesion and increased the linear localization of DSG1 in cell–cell contacts. These results suggest that DSG3 deficiency and decreased DSG1 levels in cell–cell contacts in DSG3 knockout keratinocytes (KO cells) weaken cell–cell adhesion, which may involve JNK signaling.

Materials and methods

Antibodies

The following primary antibodies were used in this study: rabbit anti-actin (A2066) antibody from Sigma-Aldrich (St. Louis, MO, USA); rabbit anti-E-cadherin (clone 24E10, #3195), mouse anti-phospho-JNK (clone G9, #9255), rabbit anti-JNK (#9252), rabbit anti-phospho-p38 MAPK (clone D3F9, #4511), and rabbit anti-p38 MAPK (clone D13E1, #8690) antibodies from Cell Signaling (San Diego, CA, USA); mouse anti-DSG1 (clone

B-11, sc-137164) antibody from Santa Cruz (Dallas, TX, USA); rabbit anti-DSG1 (24587-1-AP) and rabbit anti-DSG2 (21880-1-AP) antibodies from Proteintech (Chicago, IL, USA); mouse anti-DSG3 (clone AK9, D217-3) antibody from MBL (Tokyo, Japan); and rabbit anti-DSG3 (LS-C409947) antibody from LifeSpan BioSciences (Seattle, WA, USA).

K38 cells and cell culture medium

The murine epidermal keratinocyte cell line K38 (Reichelt and Haase 2010; Vollmers et al. 2012), originating from neonatal BALB/c mouse skin, was purchased from ECACC (Salisbury, UK). The FAD medium (Biochrom GmbH, Berlin, Germany) consists of Dulbecco's modified Eagle's medium/Ham's F12 (3.5:1.1), 50 µM calcium chloride, and 4.5 g/L D-glucose. Complete FAD medium (low-calcium medium) supplemented with 2.5% Chelex 100-treated fetal bovine serum (FBS), 0.18 mM adenine (Sigma-Aldrich), 0.5 µg/ml hydrocortisone (Sigma-Aldrich), 5 µg/ml insulin (Life Technologies, Carlsbad, CA, USA), 10^{-10} M cholera toxin (Sigma-Aldrich), 10 ng/ml epidermal growth factor (Sigma-Aldrich), 2 mM L-glutamine (Nacalai Tesque, Kyoto, Japan), and 1 mM sodium pyruvate (Wako, Osaka, Japan) was used for the growth of K38 cells. Serum calcium was removed by treating 500 mL of FBS (HyClone, South Logan, UT, USA) with 20 g of Chelex 100 (Bio-Rad Laboratories, Hercules, CA, USA) (Lichti et al. 2008). To induce cell–cell adhesion, 1.2 mM (final concentration) calcium chloride was added to the complete FAD medium.

Treatments

Cells were seeded at a density of 1.0×10^4 cells in 10-well glass slides for immunofluorescence staining or at that of 1.5×10^5 cells in 24-well plates for western blotting and dispase-based dissociation assay in a complete FAD medium. The 10-well glass slides printed with highly water-repellent marks (catalog number TF1006; Matsunami Glass Ind. Ltd., Osaka, Japan) were coated by using 0.3 mg/ml native collagen acidic solution (Cellgen I-AC; Koken, Tokyo, Japan). Cells reached confluence the next day and were cultured for the indicated times in the presence of 1.2 mM calcium to induce cell–cell adhesion. In some cases, cells were treated in a complete FAD medium containing 1.2 mM calcium (high-calcium medium) with a vehicle (dimethyl sulfoxide, DMSO) or indicated combinations of 100 nM anisomycin (Cayman Chemical, Ann Arbor, MI, USA), 20 μM BIR 796 (Cayman Chemical), and 20 μM SP600125 (Sigma-Aldrich). Anisomycin, BIRB 796, and SP600125 are an activator of both p38 MAPK and JNK, an inhibitor of p38 MAPK, and an inhibitor of JNK, and stock solutions in DMSO were prepared at concentrations of 100 μM, 10 mM, and 20 mM, respectively. The optimal concentrations of these agents for K38 cells were defined in our previous report (Nikaido et al. 2019).

Establishment of the DSG3-knockout cells (KO cells)

To disrupt the DSG3 gene in mouse K38 cells using the genome editing method, we searched for the target sequence in the DSG3 gene locus using the Optimized CRISPR Design website (http://tools.genome-engineering.org). We selected the target site at the second ATG codon in the DSG3 genomic sequence, and a pair of oligonucleotides possessing the target or complementary sequences (5′-CAC CGA TGA GAC TTA CCA TCA GGA-3′ and 5′-AAA CTC CTG ATG GTA AGT CTC ATC-3′) was inserted into the cloning site of the

pSpCas9(BB)-2A-Puro (pX459) vector (Plasmid #48139), purchased from Addgene (Cambridge, MA, USA). The construct for gene editing was designated as pX459-DSG3-207. DSG3-KO cells were produced by nucleofection of 5 μg pX459-DSG3-207 into 2 × 10^6 K38 cells (WT cells) in 100 μl of P3 primary cell solutions with the program DS-150 using a 4D-Nucleofector system (Lonza, Cologne, Germany). Nucleofected cells were seeded in a 10-cm dish in a complete FAD medium. After 24 h, the medium was replaced with one containing 2 μg/ml puromycin (InvivoGen, Sandiego, CA, USA) and cultured for 48 h. Cells were further cultured without puromycin, and the medium was changed every two days until visible colonies appeared (approximately 14 days). Candidate colonies were isolated and expanded in the complete FAD medium. To select the KO cells, candidate clones were examined with western blotting and immunofluorescence staining using an anti-DSG3 antibody.

Cloning and sequencing of the chromosomal region of the DSG3 gene in KO cells

To confirm DSG3 knockout, the target site in the genomic region was cloned and sequenced. Genomic DNA was prepared from DSG3-knockout candidate clones as described previously (Ishii et al. 2018). To amplify the flanking region of the target site for DSG3 gene disruption, genomic DNA was used as a template for PCR, using primers 5′-CAG GGC CAG CTC TTG CAC CTC TGT-3′ and 5′-GCA TGC AGA GTT CTT AGC TAT ATG-3′. The amplified DNA fragment was cloned into the pMD20-T vector (Takara Bio, Shiga, Japan) by TA cloning. Genomic sequences were determined using the M13 reverse primer (5′-CAG GAA ACA GCT ATG AC-3′) and analyzed for indel mutations near the genome-editing site.

Immunofluorescence microscopy

After washing in phosphate-buffered saline (PBS), the cells were fixed with 1% paraformaldehyde in PBS for 10 min, washed in PBS, incubated in 0.2% Triton-X 100 in PBS for 15 min, washed again in PBS, and incubated with 1% bovine serum albumin in PBS (BSA-PBS) for 30 min at room temperature to block non-specific binding. The cells were then incubated for 1 h with the indicated combinations of primary antibodies diluted in BSA-PBS. The primary antibodies used were rabbit anti-E-cadherin (1:100), mouse anti-DSG1 (1:200), rabbit anti-DSG2 (1:100), and mouse anti-DSG3 (1:200). After rinsing the cells four times with PBS, they were incubated with anti-mouse or anti-rabbit immunoglobulin conjugated with Alexa 488 or Alexa 568 (Molecular Probes, Eugene, OR, USA) at 1:400 dilution in BSA-PBS for 30 min in the dark. The sections were then washed four times with PBS and mounted in a Vectashield mounting medium containing 4′, 6-diamidino-2-phenylindole (DAPI) (Vector Laboratories, Burlingame, CA, USA). Images were obtained by sequentially scanning the specimen to prevent bleed-through using an LSM710 confocal laser scanning microscope with the ZEN 2010 software (Carl Zeiss, Oberkochen, Germany). Two objective lenses were used for confocal microscopy: Zeiss Plan-Apochromat 40×/1.3 Oil Ph3 (UV) VIS-IR and Zeiss Plan-Apochromat 100×/1.4 Oil DIC.

Gel electrophoresis and western blotting

Cells were washed thrice with ice-cold PBS and lysed with 0.2 ml of 1× lysis buffer [62.5 mM Tris (pH 6.8), 2% sodium dodecyl sulfate (SDS), 10% glycerol, 5% 2-mercaptoethanol, and 0.002% bromophenol blue)]

containing a cocktail of protease inhibitors (Sigma-Aldrich) and phosphatase inhibitors (Nacalai Tesque). Cell lysates were fractionated using SDS-polyacrylamide gel electrophoresis with 5–20% gradient gels and transferred onto polyvinylidene difluoride membranes. Precision Plus Protein Dual Color Standards (Bio-Rad, Hercules, CA, USA) were used to determine the size of the detected bands. The membranes were incubated with Blocking One (Nacalai Tesque) for 1 h and with primary antibodies for 1 h at room temperature or overnight at 4°C. Antibodies against E-cadherin (1:1,000), DSG1 (1:2,000), DSG2 (1:2,000), DSG3 (1:2,000), phospho-JNK (1:1,000), JNK (1:1,000), phospho-p38 MAPK (1:1,000), p38-MAPK (1:1,000), and actin (1:2,000) were used as primary antibodies and diluted with Tris-buffered saline (TBS) [20 mM Tris (pH 7.6) and 137 mM NaCl] containing 5% Blocking One. After washing with TBS containing 0.1% Tween 20 (T-TBS), the membranes were incubated with horseradish peroxidase-conjugated anti-rabbit or anti-mouse Ig (1:2,000) (Thermo Fisher Scientific, Waltham, MA) for 1 h. They were then washed with T-TBS, and the bands were detected using SuperSignal West Femto Maximum Sensitivity Substrate (Thermo Fisher Scientific). Some membranes were reprobed after stripping the primary and secondary antibodies with stripping buffer [62.5 mM Tris (pH 6.7), 2% SDS, and 100 mM 2-mercaptoethanol] at 50°C for 30 min.

Dispase-based dissociation assay

After washing with Hanks' balanced salt solution containing calcium and magnesium (HBSS+) (Kohjin Bio, Saitama, Japan), confluent cells cultured in a 24-well plate were incubated in a dispase solution until the whole-cell monolayer detached from the well. The dispase solution was a 1:1 mixture of 1×10^4 PU/ml dispase II

(Godo Shusei, Tokyo, Japan) in 50 mM Tris, 2 mM calcium acetate (pH 7.5), and a complete FAD medium containing 1.2 mM $CaCl_2$. The detached monolayer was washed once with HBSS+, transferred to a 1.5 ml tube containing 1 ml of HBSS+, washed once with HBSS without calcium and magnesium (Wako), and incubated for 5 min. The tube containing the cell monolayer was immediately stirred using a Voltex-Genie 2 Mixer (M&S Instruments, Osaka, Japan) at maximal speed for 5 s. To prevent further dissociation, 60 μl of 20% paraformaldehyde solution was added to the tube. The solution containing the cell fragments was transferred to 24-well plates and the number of fragments was counted.

Statistical analysis

All data are expressed as the mean ± standard error of the mean. One-way analysis of variance (ANOVA) and Tukey's test were used for statistical evaluations. Statistical significance was set as $*p < 0.05$, $**p < 0.01$, and $***p < 0.001$.

Results

Genomic editing for DSG3 gene disruption in K38 cells

To verify the loss of DSG3 gene expression in two of the clones (clone 207-4 and clone 207-46), we performed western blotting and immunofluorescence staining with an anti-DSG3 antibody (Figs. 1–3). These results show that DSG3 proteins completely disappeared from the cells of the two clones. We also performed genomic analyses of the two clones (Table 1). These genomic analyses showed that clone 207-4 carried an insertion

mutation (T) at upstream of second ATG codon or a deletion (7 nt) at between first and second ATG codon. Clone 207-46 possessed two types of indel mutation (T insertion or G deletion) at upstream of target site or two deletion type mutation (13 nt deletion at between first and second ATG codon or 181 nt deletion at upstream of first ATG codon). These mutations caused by genome editing lead frame-shift in coding region of DSG3 gene and loss of normal gene expression. Therefore, these two clones are considered DSG3 knockout cells (KO cells).

The localization of DSG1 and DSG2 gets downregulated in cell–cell contacts of KO cells

To understand the role of DSG3 in desmosomes, which are formed by a mixture of desmosomal cadherins, including DSG1, DSG2, and DSG3, we first investigated the localization of desmosomal cadherins and E-cadherin in WT and KO cells (clone 207-4) cultured for one day in a high-calcium medium (Fig. 1). Intense linear staining for DSG1 was detected in cell–cell contacts in WT cells (Fig. 1a), whereas faint DSG1 staining (Fig. 1d, arrowheads) and intense E-cadherin staining (Fig. 1e, arrowheads) were observed in KO cells. Several cells growing on top of the monolayer of WT (Fig. 1a) and KO (Fig. 1d) cells showed strong DSG1 staining. Compared to DSG1 staining in cell–cell contacts in WT cells (Fig. 1a), DSG2 staining was heterogeneous and weak in WT cells (Fig. 1h) and very weak in KO cells (Fig. 1k). DSG3 staining was not detected in KO cells (Fig. 1j), indicating the loss of DSG3 proteins. No clear difference was observed in E-cadherin staining between WT (Fig. 1b) and KO (Fig. 1e) cells. Considering that the localization of DSG1 to cell–cell contacts may be delayed or suppressed in KO cells, we further investigated the localization of DSG1 in KO cells (clone 207-4) cultured for three days (Fig. 2). Some DSG1 staining in cell–cell contacts, which showed intense E-cadherin

staining (Fig. 2e, arrowheads), was still faint (Fig. 2d, arrowheads) in KO cells compared to WT cells (Fig. 2a). Several cell clusters (asterisks in Figs. 2g–i) with gaps between adjacent cells, as judged by the loss of DSG1 (Fig. 2g) and E-cadherin (Fig. 2h) staining, were occasionally observed. DSG2 staining of cell–cell contacts in KO cells (Fig. 2n) was almost identical to that in WT cells (Fig. 2k). Negative controls for immunofluorescence are shown in Supplementary Fig. 1. Another clone (207-46) showed similar results (Supplementary Fig. 2).

Loss of the DSG3 protein does not activate stress-activated MAPKs

Next, we investigated the protein expression levels of DSG1, DSG2, DSG3, and E-cadherin and the phosphorylation of p38 MAPK and JNK with western blotting (Fig. 3). DSG1 expression increased in KO cells (clone 207-4) cultured for one and three days compared to that in WT cells. DSG2 expression in KO cells cultured for one day, but not three days, increased compared to that in WT cells. DSG3 was not detected in the KO cells cultured for one or three days. There was no difference in E-cadherin protein levels between WT and KO cells on days 1 and 3. As it has been reported that p38 MAPK was activated in DSG3 knockdown or deletion cells (Hartlieb et al. 2014; Rötzer et al. 2016), we investigated stress-activated MAPKs (p38 MAPK and JNK). We did not find any differences in p38 MAPK phosphorylation in WT and KO cells, although p38 MAPK phosphorylation in both WT and KO cells increased when cultured for three days compared to one day. JNK phosphorylation was not observed.

Loss of DSG3 impairs cell–cell adhesion over time

To examine the strength of intercellular junctions, we performed a dispase-based dissociation assay (Fig. 4). The WT cell sheets cultured for one and three days did not fragment. KO cell (clone 207-4) sheets cultured for one and three days yielded 32.00 ± 7.81 and 141.33 ± 21.74 fragments, respectively, indicating that cell–cell adhesion in KO cells gets impaired over time.

The linear localization of DSG1 to cell–cell contacts is promoted by the inhibition of JNK in KO cells but inhibited by the activation of JNK in WT cells

We previously reported that the activation of JNK, but not p38 MAPK, delayed the localization of claudins, tight junction membrane proteins, to cell–cell contacts in WT cells 6 h after the induction of intercellular junction formation by high calcium levels (Nikaido et al. 2019). Therefore, we investigated whether stress-activated MAPKs affect the localization of DSG1 in cell–cell contacts during the early stages of cell–cell junction formation in KO cells (clone207-4). KO cells (Figs. 5a, e) formed DSG1-negative, DSG1-positive zipper-like (arrow), or DSG1-positive linear (arrowhead) cell–cell contacts 6 h after the addition of 1.2 mM calcium, while most of the WT cells (Figs. 5d, h) formed DSG1-positive linear cell–cell contacts (arrowheads). The localization of DSG1 in p38 MAPK-inhibited KO cells (Figs. 5b, f) was similar to that in KO cells (Figs. 5a, e), but DSG1-positive cell–cell contacts slightly increased. The treatment of KO cells with the JNK inhibitor (Figs. 5c, g) promoted the linear localization of DSG1 in cell–cell contacts (arrowhead), as seen in WT cells (Figs. 5d, h). DSG1 localization in cell–cell contacts in WT cells treated with anisomycin (activation of both p38 MAPK and JNK; Fig. 5i), anisomycin plus BIRB796 (activation of JNK; Fig. 5j), or anisomycin plus SP600125 (activation

of p38 MAPK; Fig. 5k) resembled that in KO cells treated with the vehicle (Fig. 5a, e), BIRB 796 (Figs. 5b, f), or SP600125 (Figs. 5c, g), respectively. These results indicate that concerning DSG1 localization in cell–cell contacts, KO cells resemble WT cells, in which JNK or both JNK and p38 MAPK are activated. We validated the specificity of BIRB 796 and SP600125 in KO cells (clone207-4) (Supplementary Fig. 3) and WT cells previously (Nikaido et al. 2019). Phosphorylation of p38 MAPK and JNK increased due to anisomycin treatment. BIRB 796 and SP600125 downregulated the phosphorylation of p38 MAPK and JNK, respectively. Clone 207-46 showed similar results (Supplementary Fig. 4).

The inhibition of JNK enhances cell–cell adhesion more than that of p38 MAPK

To investigate the effect of p38 MAPK and JNK inhibition on the strength of intercellular junctions in KO cell monolayers, we performed a dispase-based dissociation assay (Fig. 6). KO cells (clone207-4) cultured for 24 h with 1.2 mM calcium (Ca), Ca plus BIRB 796, or Ca plus SP600125 yielded fragments of 32.33 ± 7.33, 15.33 ± 2.63, and 7.20 ± 2.89, respectively, suggesting that the inhibition of JNK enhances cell–cell adhesion more than that of p38 MAPK. Inhibition of JNK also enhanced cell–cell adhesion in clone 207-46 (Supplementary Fig. 5).

Discussion

In this study, we found that the disruption of the DSG3 gene in K38 cells reduced the linear localization of DSG1 to cell–cell contacts and impaired cell–cell adhesion over time without the apparent activation of stress-activated MAPKs. The linear localization of DSG1 to cell–cell contacts and the strength of cell–cell adhesion were

promoted by the pharmacological inhibition of JNK rather than p38 MAPK in KO cells. Conversely, pharmacological activation of JNK, but not p38 MAPK, in WT cells reduced the linear localization of DSG1 in cell–cell contacts. Our data indicate that DSG1 and DSG2 in KO cells cannot compensate for the attenuation of cell–cell adhesion strength caused by DSG3 deficiency. While patients with genetic loss of DSG3 appear to be rare, they exhibit blisters in the oral and laryngeal mucosa, but not in the epidermis (Kim et al. 2019). This report supports our finding that other DSGs do not always compensate for the loss of DSG3. The inhibition of JNK signaling may enhance cell–cell adhesion in patients with genetic loss of DSG3, although we have not yet demonstrated a direct link between the loss of DSG3 and the activation of JNK signaling.

Immunofluorescence staining showed that DSG1 and DSG2 localization in cell–cell contacts in KO cells decreased on day 1 after the addition of calcium compared with WT cells, but only DSG2 was able to localize to cell–cell contacts on day 3. Dissociation assays demonstrated that cell–cell adhesions in the monolayers of KO cells were weaker than those in WT cells on day 1 and were further weakened on day 3. These results suggest that the loss of DSG3 and the reduced localization of DSG1, rather than DSG2, in cell–cell contacts may be related to the weakening of cell–cell adhesion. This assumption is supported by previous reports described below. A dissociation assay showed that DSG1-knockdown HaCaT cells by siRNA yielded 9.6 times more fragments than DSG2-knockdown cells (Hartlieb et al. 2014) and that DSG2-knockdown HaCaT cells did not impair cell–cell adhesion under conditions of low shear (Hartlieb et al. 2013). Keratinocytes derived from DSG3 knockout mice and DSG3-knockdown HaCaT cells produced 21.4 times and 6.3 times more fragments, respectively, than control cells (Hartlieb et al. 2014). Cell–cell adhesion was impaired in DSG3-deficient

keratinocytes (Baron et al. 2012). In patients with pemphigus who develop autoantibodies against DSG1 and/or DSG3, DSG1- and DSG3-mediated cell–cell adhesion is disrupted, leading to the formation of blisters within the epidermis and mucous membranes (Mahoney et al. 1999; Shirakata et al. 1998; Stanley and Amagai 2006; Waschke and Spindler 2014). The formation of blisters by suprabasilar acantholysis in DSG3 knockout mice indicates that DSG3 deficiency weakens cell–cell adhesion (Koch et al. 1997). Exogenous expression of DSG1 in DSG3 knockout mice compensates for cell–cell adhesion (Hanakawa et al. 2002). Therefore, the loss of DSG3 and reduction of DSG1 in cell–cell contacts may impair cell–cell adhesion in KO cells. The dissociation assay showed that cell–cell adhesion in KO cells on day 3 was weaker than that on day 1. Some clusters of KO cells with gaps between adjacent cells (Figs. 2g–i) may be related to the weakening of cell–cell adhesion on day 3.

K38 cells cultured on the membranes of cell culture inserts form stratified epithelium under the airlift condition (Nikaido et al. 2019; Ishikawa et al. 2022). Therefore, some cells could grow on top of monolayers of WT and KO cells when cultured on culture dishes. These cells formed small cell clusters of fewer than 10 cells on top of monolayers and showed a periphery without cell–cell contacts. We speculate that DSG1 protein synthesis is upregulated when cells move to the surface of the monolayer and form E-cadherin-based cell–cell contacts with adjacent cells. Subsequently, DSG1 may be transported from the cytoplasm to cell–cell contacts to form desmosomes, and DSG1 protein synthesis may be gradually downregulated when cell–cell contacts are formed around the entire cell periphery. Single cells on top of monolayers (arrows in Supplementary Fig. 2a) that were not in contact with other surface cells often showed very strong DSG1 staining in the cytoplasm. On the other hand, cell clusters on top of monolayers that adhered to each other showed strong, moderate, or weak

DSG1 staining in the cytoplasm and cell–cell contacts (Supplementary Figs. 2a and 2g). These results suggested that DSG1 staining intensity in the cytoplasm decreased during cell adhesion formation and maturation process. The significance of these cells with strong DSG1 staining needs further investigation.

We speculated that the reduced localization of DSG1 in cell–cell contacts was due to decreased expression of the DSG3 protein, inhibition of trafficking of DSG1 to the plasma membrane, and/or instability (accelerated degradation) of DSG1 in plasma membranes. In the early stage of cell–cell junction formation by the addition of calcium in K38 cells, dotted or zipper-like staining for ZO-1, a tight junction-associated peripheral membrane protein, was detected in cell–cell contacts at 2 h, gradually replaced with linear staining at 6 h, and completely replaced at 12 h, suggesting the maturation of cell–cell junctions (Nikaido et al. 2019). Based on these observations, we examined the localization of DSG1 6 h after the addition of calcium in WT and KO cells. Linear localization of DSG1 in cell–cell contacts was observed in WT cells, whereas negative, zipper-like, or linear localization of DSG1 was detected in KO cells. On day 3, DSG1 staining in cell–cell contacts in KO cells remained faint compared to that in WT cells. Unexpectedly, the protein expression levels of DSG1 in KO cells on days 1 and 3 were higher than those in WT cells, as shown by western blotting. As the protein expression levels of DSG1 increase in the KO cells, DSG1 protein transport to plasma membranes may be inhibited. In contrast to our findings, DSG3-deficient keratinocytes exhibited normal membrane localization of DSG1 and increased protein levels of DSG1 despite weakened cell–cell adhesion (Baron et al. 2012). This discrepancy may be due to differences in the cells (primary cells vs. cell lines) used in the experiments.

E-cadherin plays a central role in cell–cell junction formation in epithelial cells. This is evidenced by

the fact that the depletion of extracellular Ca^{2+} induces the loss of adherens junctions, followed by the loss of desmosomes and tight junctions. Expression of a dominant-negative mutant of N-cadherin (Amagai et al. 1995) or E-cadherin (Zhu and Watt 1996) disrupts both adherens junctions and desmosomes. The inhibition of adherens junction formation by antibodies against E- and P-cadherin inhibits desmosome formation (Lewis et al. 1994). PC9 cells, which express E-cadherin and β-catenin but no α-catenin, do not form cell–cell junctions. Expression of α-catenin in PC9 cells restored the formation of adherence junctions and induced the formation of desmosomes and tight junctions (Watabe et al. 1994). After adherens junction formation, desmocollin aids in initiating desmosome formation (Hanakawa et al. 2000). These findings indicate that the formation of adherens junctions is a prerequisite for desmosome formation and that adherens junctions are required to maintain desmosomes. In this study, E-cadherin localization in cell–cell contacts was not altered in KO cells, as shown by immunostaining. The downregulated localization of DSG1 to cell–cell contacts appears to be due to factors other than E-cadherin.

We did not detect the activation of JNK in WT or KO cells, nor did we detect increased activation of p38 MAPK in KO cells compared to WT cells. In contrast to our findings, p38 MAPK is activated in DSG3 knockdown HaCaT cells (Hartlieb et al. 2014) or DSG3 knockout mice (Rötzer et al. 2016). As the binding of PV IgG to keratinocytes transiently activates p38 MAPK after 240 min (Chernyavsky et al. 2007), p38 MAPK and JNK may be transiently activated in KO cells at specific time points that were not examined. As the activation of JNK in K38 cells delayed the localization of tight junction proteins such as ZO-1 and claudins in cell–cell contacts and maturation of cell–cell junctions from a zipper-like to linear appearance (Nikaido et al.

2019), we investigated whether the activation of stress-activated MAPKs using indicated combinations of anisomycin, BIRB 796, and SP600125 affects the localization of DSG1 in cell–cell contacts and the strength of cell–cell adhesion in KO and WT cells. The inhibition of JNK, but not p38 MAPK, in KO cells promoted the linear localization of DSG1 in cell–cell contacts. Conversely, the activation of JNK, regardless of p38 MAPK activation, reduced the localization of DSG1 in cell–cell contacts in WT cells. WT cells treated with anisomycin and SP600125, in which p38 MAPK was activated and JNK was inhibited, promoted the linear localization of DSG1. These results suggest that JNK activation inhibits the linear localization of DSG1 at cell–cell contacts in both WT and KO cells. Furthermore, dissociation assays demonstrated that the inhibition of JNK enhanced cell–cell adhesion in KO cells compared to the inhibition of p38 MAPK. Taken together, the inhibition of JNK promotes the linear localization of DSG1 in cell–cell contacts and enhances cell–cell adhesion in KO cells.

Conclusions

In conclusion, the disruption of the DSG3 gene in K38 cells weakens cell–cell adhesion and concomitantly reduces the linear localization of DSG1 to cell–cell contacts. Cell–cell adhesion in KO cells is promoted by the pharmacological inhibition of JNK signaling and concomitantly increases the linear localization of DSG1 to cell–cell contacts. Inhibition of JNK signaling may improve cell–cell adhesion in diseases in which DSG3 expression is impaired.

Author contributions T.I.[1] (T. Inai) conceived and planned the experiments. T.I.[1] and T.I.[2] (T. Ishii) established

DSG3 KO cells. S.O. carried out all experiments with help from T.O., Y.I., T.M., and T.I.[1], and T.I.[1] contributed to the interpretation of the results. Y.I. analyzed data of dispase-based dissociation assay. All authors read and approved the final manuscript. T.I.[1] wrote the manuscript with input from all authors and supervised the project.

Data availability The datasets generated and analyzed during the current study are available from the corresponding authors on reasonable request.

Declarations

Conflict of interest The authors declare that they have no conflict of interest.

References

Amagai M, Fujimori T, Masunaga T, Shimizu H, Nishikawa T, Shimizu N, Takeichi M, Hashimoto T (1995) Delayed assembly of desmosomes in keratinocytes with disrupted classic-cadherin-mediated cell adhesion by a dominant negative mutant. J Invest Dermatol 104 (1):27–32. https://doi.org/10.1111/1523-1747.ep12613462

Amagai M, Stanley JR (2012) Desmoglein as a target in skin disease and beyond. J Invest Dermatol 132 (3 Pt. 2):776–784. https://doi.org/10.1038/jid.2011.390

Aono S, Hirai Y (2008) Phosphorylation of claudin-4 is required for tight junction formation in a human keratinocyte cell line. Exp Cell Res 314 (18):3326–3339. https://doi.org/10.1016/j.yexcr.2008.08.012

Baron S, Hoang A, Vogel H, Attardi LD (2012) Unimpaired skin carcinogenesis in desmoglein 3 knockout mice. PLOS ONE 7 (11):e50024. https://doi.org/10.1371/journal.pone.0050024

Berkowitz P, Hu P, Liu Z, Diaz LA, Enghild JJ, Chua MP, Rubenstein DS (2005) Desmosome signaling. Inhibition of p38MAPK prevents pemphigus vulgaris IgG-induced cytoskeleton reorganization. J Biol Chem 280 (25):23778–23784. https://doi.org/10.1074/jbc.M501365200

Berkowitz P, Hu P, Warren S, Liu Z, Diaz LA, Rubenstein DS (2006) P38MAPK inhibition prevents disease in pemphigus vulgaris mice. Proc Natl Acad Sci U S A 103 (34):12855–12860. https://doi.org/10.1073/pnas.0602973103

Bogoyevitch MA, Court NW (2004) Counting on mitogen-activated protein kinases--ERKs 3, 4, 5, 6, 7 and 8. Cell Signal 16 (12):1345–1354. https://doi.org/10.1016/j.cellsig.2004.05.004

Chernyavsky AI, Arredondo J, Kitajima Y, Sato-Nagai M, Grando SA (2007) Desmoglein versus non-desmoglein signaling in pemphigus acantholysis: characterization of novel signaling pathways downstream of pemphigus vulgaris antigens. J Biol Chem 282 (18):13804–13812. https://doi.org/10.1074/jbc.M611365200

Delva E, Tucker DK, Kowalczyk AP (2009) The desmosome. Cold Spring Harb Perspect Biol 1 (2):a002543. https://doi.org/10.1101/cshperspect.a002543

Garcia MA, Nelson WJ, Chavez N (2018) Cell-cell junctions organize structural and signaling networks. Cold Spring Harb Perspect Biol 10 (4). https://doi.org/10.1101/cshperspect.a029181

Garrod D, Chidgey M (2008) Desmosome structure, composition and function. Biochim Biophys Acta 1778

(3):572–587. https://doi.org/10.1016/j.bbamem.2007.07.014

Hagemann C, Blank JL (2001) The ups and downs of MEK kinase interactions. Cell Signal 13 (12):863–875. https://doi.org/10.1016/s0898-6568(01)00220-0

Hanakawa Y, Amagai M, Shirakata Y, Sayama K, Hashimoto K (2000) Different effects of dominant negative mutants of desmocollin and desmoglein on the cell-cell adhesion of keratinocytes. J Cell Sci 113 (10):1803–1811. https://doi.org/10.1242/jcs.113.10.1803

Hanakawa Y, Matsuyoshi N, Stanley JR (2002) Expression of desmoglein 1 compensates for genetic loss of desmoglein 3 in keratinocyte adhesion. J Invest Dermatol 119 (1):27–31. https://doi.org/10.1046/j.1523-1747.2002.01780.x

Hartlieb E, Kempf B, Partilla M, Vigh B, Spindler V, Waschke J (2013) Desmoglein 2 is less important than desmoglein 3 for keratinocyte cohesion. PLOS ONE 8 (1):e53739. https://doi.org/10.1371/journal.pone.0053739

Hartlieb E, Rötzer V, Radeva M, Spindler V, Waschke J (2014) Desmoglein 2 compensates for desmoglein 3 but does not control cell adhesion via regulation of p38 mitogen-activated protein kinase in keratinocytes. J Biol Chem 289 (24):17043–17053. https://doi.org/10.1074/jbc.M113.489336

Ishii T, Hayakawa H, Igawa T, Sekiguchi T, Sekiguchi M (2018) Specific binding of PCBP1 to heavily oxidized RNA to induce cell death. Proc Natl Acad Sci U S A 115 (26):6715–6720. https://doi.org/10.1073/pnas.1806912115

Ishikawa S, Nikaido M, Otani T, Ogata K, Iida H, Inai Y, Tamaoki S, Inai T (2022) Inhibition of retinoid X

receptor improved the morphology, localization of desmosomal proteins and paracellular permeability in three-dimensional cultures of mouse keratinocytes. Microscopy 71 (3):152–160. https://doi.org/10.1093/jmicro/dfac007

Kim JH, Kim SE, Park HS, Lee SH, Lee SE, Kim SC (2019) A homozygous nonsense mutation in the DSG3 gene causes acantholytic blisters in the oral and laryngeal mucosa. J Invest Dermatol 139 (5): 1187–1190. https://doi.org/10.1016/j.jid.2018.09.038

Kitagawa N, Inai Y, Higuchi Y, Iida H, Inai T (2014) Inhibition of JNK in HaCaT cells induced tight junction formation with decreased expression of cytokeratin 5, cytokeratin 17 and desmoglein 3. Histochem Cell Biol 142 (4):389–399. https://doi.org/10.1007/s00418-014-1219-9

Koch PJ, Mahoney MG, Ishikawa H, Pulkkinen L, Uitto J, Shultz L, Murphy GF, Whitaker-Menezes D, Stanley JR (1997) Targeted disruption of the pemphigus vulgaris antigen (desmoglein 3) gene in mice causes loss of keratinocyte cell adhesion with a phenotype similar to pemphigus vulgaris. J Cell Biol 137 (5):1091–1102. https://doi.org/10.1083/jcb.137.5.1091

Kojima T, Fuchimoto J, Yamaguchi H, Ito T, Takasawa A, Ninomiya T, Kikuchi S, Ogasawara N, Ohkuni T, Masaki T, Hirata K, Himi T, Sawada N (2010) C-Jun N-terminal kinase is largely involved in the regulation of tricellular tight junctions via tricellulin in human pancreatic duct epithelial cells. J Cell Physiol 225 (3):720–733. https://doi.org/10.1002/jcp.22273

Kyriakis JM, Avruch J (2001) Mammalian mitogen-activated protein kinase signal transduction pathways activated by stress and inflammation. Physiol Rev 81 (2):807–869.

https://doi.org/10.1152/physrev.2001.81.2.807

Lewis JE, Jensen PJ, Wheelock MJ (1994) Cadherin function is required for human keratinocytes to assemble desmosomes and stratify in response to calcium. J Invest Dermatol 102 (6):870–877. https://doi.org/10.1111/1523-1747.ep12382690

Lichti U, Anders J, Yuspa SH (2008) Isolation and short-term culture of primary keratinocytes, hair follicle populations and dermal cells from newborn mice and keratinocytes from adult mice for in vitro analysis and for grafting to immunodeficient mice. Nat Protoc 3 (5):799–810. https://doi.org/10.1038/nprot.2008.50

Mahoney MG, Wang Z, Rothenberger K, Koch PJ, Amagai M, Stanley JR (1999) Explanations for the clinical and microscopic localization of lesions in pemphigus foliaceus and vulgaris. J Clin Invest 103 (4):461–468. https://doi.org/10.1172/JCI5252

Minakami M, Kitagawa N, Iida H, Anan H, Inai T (2015) p38 mitogen-activated protein kinase and c-Jun NH2-terminal protein kinase regulate the accumulation of a tight junction protein, ZO-1, in cell-cell contacts in HaCaT cells. Tissue Cell 47 (1):1–9. https://doi.org/10.1016/j.tice.2014.10.001

Naydenov NG, Hopkins AM, Ivanov AI (2009) C-Jun N-terminal kinase mediates disassembly of apical junctions in model intestinal epithelia. Cell Cycle 8 (13):2110–2121. https://doi.org/10.4161/cc.8.13.8928

Nikaido M, Otani T, Kitagawa N, Ogata K, Iida H, Anan H, Inai T (2019) Anisomycin, a JNK and p38 activator, suppresses cell-cell junction formation in 2D cultures of K38 mouse keratinocyte cells and reduces

claudin-7 expression, with an increase of paracellular permeability in 3D cultures. Histochem Cell Biol 151 (5):369–384. https://doi.org/10.1007/s00418-018-1736-z

Pearson LL, Castle BE, Kehry MR (2001) CD40-mediated signaling in monocytic cells: up-regulation of tumor necrosis factor receptor-associated factor mRNAs and activation of mitogen-activated protein kinase signaling pathways. Int Immunol 13 (3):273–283. https://doi.org/10.1093/intimm/13.3.273

Reichelt J, Haase I (2010) Establishment of spontaneously immortalized keratinocyte lines from wild-type and mutant mice. Methods Mol Biol 585:59–69. https://doi.org/10.1007/978-1-60761-380-0_5

Rötzer V, Hartlieb E, Winkler J, Walter E, Schlipp A, Sardy M, Spindler V, Waschke J (2016) Desmoglein 3-dependent signaling regulates keratinocyte migration and wound healing. J Invest Dermatol 136 (1):301–310. https://doi.org/10.1038/JID.2015.380

Schaeffer HJ, Weber MJ (1999) Mitogen-activated protein kinases: specific messages from ubiquitous messengers. Mol Cell Biol 19 (4):2435–2444. https://doi.org/10.1128/MCB.19.4.2435

Shirakata Y, Amagai M, Hanakawa Y, Nishikawa T, Hashimoto K (1998) Lack of mucosal involvement in pemphigus foliaceus may be due to low expression of desmoglein 1. J Invest Dermatol 110 (1):76–78. https://doi.org/10.1046/j.1523-1747.1998.00085.x

Siljamäki E, Raiko L, Toriseva M, Nissinen L, Näreoja T, Peltonen J, Kähäri VM, Peltonen S (2014) p38delta mitogen-activated protein kinase regulates the expression of tight junction protein ZO-1 in differentiating human epidermal keratinocytes. Arch Dermatol Res 306 (2):131–141. https://doi.org/10.1007/s00403-013-1391-0

Stanley JR, Amagai M (2006) Pemphigus, bullous impetigo, and the staphylococcal scalded-skin syndrome. N Engl J Med 355 (17):1800–1810. https://doi.org/10.1056/NEJMra061111

Vollmers A, Wallace L, Fullard N, Höher T, Alexander MD, Reichelt J (2012) Two- and three-dimensional culture of keratinocyte stem and precursor cells derived from primary murine epidermal cultures. Stem Cell Rev Rep 8 (2):402–413. https://doi.org/10.1007/s12015-011-9314-y

Waschke J, Spindler V (2014) Desmosomes and extradesmosomal adhesive signaling contacts in pemphigus. Med Res Rev 34 (6):1127–1145. https://doi.org/10.1002/med.21310

Watabe M, Nagafuchi A, Tsukita S, Takeichi M (1994) Induction of polarized cell-cell association and retardation of growth by activation of the E-cadherin-catenin adhesion system in a dispersed carcinoma line. J Cell Biol 127 (1):247–256. https://doi.org/10.1083/jcb.127.1.247

Zhu AJ, Watt FM (1996) Expression of a dominant negative cadherin mutant inhibits proliferation and stimulates terminal differentiation of human epidermal keratinocytes. J Cell Sci 109 (13):3013–3023. https://doi.org/10.1242/jcs.109.13.3013

Table 1 Frequency of mutation types in DSG3 genome editing

Clone	type of mutation	number of events / number of clones sequenced
207-4	insertion (T)	13/14
	deletion (7 nt)	1/14
207-46	insertion (T)	3/16
	deletion (G)	4/16
	deletion (13 nt)	3/16
	deletion (181 nt)	6/16

Figure legends

Fig. 1 The localization of DSG1 and DSG2 decreases in cell–cell contacts of KO cells cultured for one day. Confluent WT (a–c, g–i) and KO (d–f, j–l) cells were cultured for one day in the presence of 1.2 mM calcium. Cells were double-stained with antibodies against either DSG1 (a, d, green) and E-cadherin (Ecad) (b, e, red) or DSG3 (g, j, green) and DSG2 (h, k, red). Merged images are shown in c, f, i, and l. Nuclei were stained with DAPI (c, f, i, l, blue). Several cells growing on top of a monolayer of WT (a) or KO (d) cells show heavy staining for DSG1. Arrowheads indicate cell–cell contacts that had faint staining for DSG1 (d) but intense staining for Ecad (e). DSG3 was localized to cell–cell contacts in WT cells (g) but was not detected in KO cells (j). DSG2 staining in cell–cell contacts in KO cells (k) is faint compared with that in WT cells (h). Scale bar: 20 μm.

Fig. 2 Decreased DSG1 levels in cell–cell contacts in KO cells persist for three days. Confluent WT (a–c, j–l) and KO (d–i, m–o) cells were cultured for three days in the presence of 1.2 mM calcium. Cells were double-stained with antibodies against either DSG1 (a, d, g, green) and Ecad (b, e, h, red) or DSG3 (j, m, green) and DSG2 (k, n, red). Merged images are shown in c, f, i, l, and o. Nuclei were stained with DAPI (c, f, i, l, o, blue). Arrowheads indicate cell–cell contacts that had faint staining for DSG1 (d) but intense staining for Ecad (e). Occasionally, a KO cell (asterisk in g–i) with an intact nucleus but no DSG1 or E-cadherin staining would be found. As shown by E-cadherin staining, cells surrounding the asterisk-indicated cell (h) have gaps between adjacent cells. Several cells growing on top of a monolayer of WT cells (a, j) and KO cells (d, g) show heavy staining for DSG1 (a, d, g) and DSG3 (j). DSG3 was localized in cell–cell contacts in WT cells (j) but was not detected in KO cells (m). DSG2 was detected in cell–cell contacts of KO cells (n) and those of WT cells (k). Scale bar: 20 μm.

Fig. 3 DSG3 protein levels increased but the phosphorylation of JNK and p38 MAPK did not increase in KO cells. Confluent WT and KO cells were cultured for one or three days in the presence of 1.2 mM calcium. Total cell lysates were separated by SDS-PAGE, followed by western blotting with antibodies to DSG1, DSG2, DSG3, E-cadherin (Ecad), phospho-p38 MAPK (P-p38), p38 MAPK (p38), phospho-JNK (P-JNK), JNK, and actin. DSG1 (one and three days) and DSG2 (one day) immunoreactivity increased in KO cells compared with WT cells. DSG3 immunoreactivity was not detected in the KO cells. The E-cadherin immunoreactivity of both the

WT and KO cells slightly decreased on day 3. The P-p38 MAPK immunoreactivity of both the WT and KO cells increased on day 3. There is no apparent difference in the P-p38 immunoreactivity in the WT and KO cells at days 1 and 3 d. P-JNK immunoreactivity was not detected.

Fig. 4 Cell–cell adhesion in KO cells became impaired over time. Confluent WT and KO cells were cultured for one or three days in the presence of 1.2 mM calcium. Cell monolayers were detached from 24-well plates by dispase, transferred to 1.5 ml tubes, vortexed, and transferred to 24-well plates. Representative images of WT and KO cell monolayers **s**ubjected to dispase-based dissociation assays are shown. The number of cell monolayer fragments was counted (n = 6). WT cell monolayers cultured for one or three days did not fragment. KO cell monolayers cultured for three days yielded 4.4 times more fragments than those cultured for one day. WT_1: WT cells cultured for one day, KO_1: KO cells cultured for one day, WT_3: WT cells cultured for three days, KO_3: KO cells cultured for three days. Statistical significance was set as $*p < 0.05$, $**p < 0.01$, and $***p < 0.001$. ns: not significant.

Fig. 5 Linear localization of DSG1 to cell–cell contacts is promoted by JNK inhibition in KO cells and conversely inhibited by JNK activation in WT cells. Confluent KO cells were cultured for 6 h in a high-calcium medium with a vehicle (a, e), 20 μM BIRB 796 (b, f), or 20 μM SP600125 (c, g). Confluent WT cells were cultured for 6 h in a high-calcium medium with a vehicle (d, h), 100 nM anisomycin (i), 100 nM anisomycin plus 20 μM BIRB 796 (j), or 100 nM anisomycin plus 20 μM SP600125 (k). Cells were stained with an antibody

against DSG1. In WT cells (d, h), intense linear immunoreactivity for DSG1 (arrowheads) was detected in most of the cell–cell contacts. In contrast to WT cells, negative, faint, zipper-like (a, e, arrow), or linear (a, e, arrowhead) immunoreactivity for DSG1 was detected in cell–cell contacts in KO cells. BIRB 796 treatment slightly promoted zipper-like (b, f, arrow) or linear (b, f, arrowhead) localization of DSG1 to cell–cell contacts in KO cells. SP600125 treatment promoted the linear localization of DSG1 to cell–cell contacts in KO cells (c, g, arrowhead). DSG1 localization in cell–cell contacts in WT cells treated with anisomycin (i), anisomycin plus BIRB796 (j), and anisomycin plus SP600125 (k) resembles that in KO cells treated with a vehicle (a, e), BIRB 796 (b, f), and SP600125 (c, g), respectively. Scale bars in a–d, e–h, and i–k: 20 μm, 10 μm, and 20 μm, respectively.

Fig. 6 The inhibition of JNK restores cell–cell adhesion better than the inhibition of p38 MAPK in KO cells. Confluent KO cells were cultured for 24 h in the presence of 1.2 mM calcium (Ca), Ca plus 20 μM BIRB 796 (BIRB), or Ca plus 20 μM SP600125 (SP). Cell monolayers were detached from 24-well plates by dispase, transferred to 1.5 ml tubes, vortexed, and transferred to 24-well plates. Representative images of KO cell monolayers subjected to dispase-based dissociation assays after a 24-h treatment of BIRB 796 or SP600125 are shown. The number of cell monolayer fragments was counted (n = 6). Compared to the control, the number of fragments was reduced by 52.6% or 77.7% with BIRB or SP treatment, respectively. Statistical significance was set as $*p < 0.05$, $**p < 0.01$, and $***p < 0.001$. ns: not significant.

Supplementary Fig. 1 Negative controls for immunofluorescence. Confluent WT (a, b) and KO (c, d) cells were cultured for one day (a, c) or three days (b, d) in the presence of 1.2 mM calcium. Confluent KO cells were cultured for 6 h in a high-calcium medium with a vehicle (e), 20 μM BIRB 796 (f), or 20 μM SP600125 (g). Confluent WT cells were cultured for 6 h in a high-calcium medium with a vehicle (h), 100 nM anisomycin (i), 100 nM anisomycin plus 20 μM BIRB 796 (j), or 100 nM anisomycin plus 20 μM SP600125 (k). They were incubated with a mixture of anti-mouse and anti-rabbit immunoglobulin conjugated with Alexa 488 or Alexa 568, omitting the primary antibodies. Nuclei were stained with DAPI, and merged images are shown. No specific immunofluorescence was observed. Scale bar: 20 μm.

Supplementary Fig. 2 The localization of DSG1 decreases in cell–cell contacts of KO cells cultured for one and three days. Confluent KO cells (clone 207-46) were cultured for one (a–f) and three (g–l) days in the presence of 1.2 mM calcium. Cells were double-stained with antibodies against either DSG1 (a, g, green) and E-cadherin (Ecad) (b, h, red) or DSG3 (d, j, green) and DSG2 (e, k, red). Merged images are shown in c, f, i, and l. Nuclei were stained with DAPI (c, f, i, l, blue). After one day of culture, some cell clusters growing on top of the KO cell monolayer (hereafter referred to as surface cells) showed weak to moderate DSG1 staining in the cytoplasm and cell–cell contacts (asterisks in a), while cells that adhered to the glass slides (hereafter referred to as basal cells) showed weak DSG1 staining (a). Arrowheads indicate cell–cell contacts between basal cells that had faint staining for DSG1 (a) but intense staining for Ecad (b). Two single cells (arrows in a) on top of the KO cell monolayer that were not in contact with other surface cells showed very strong DSG1 staining in the cytoplasm

(a). DSG3 staining was not detected in KO cells (d). DSG2 staining in cell–cell contacts (e) was heterogeneous and weak. After three days of culture, the area of surface cell clusters increased, and surface cells showed weak to strong DSG1 staining in the cytoplasm (g). Occasionally, some gaps (asterisks in g–i) were observed between basal cells. These gaps were visible thorough three surface cells with weak to moderate cytoplasmic DSG1 staining (outlined by arrowheads in g). DSG3 staining was not detected in KO cells (j). Compared to one day of culture, DSG2 staining in cell–cell contacts was slightly stronger (k). Scale bar: 20 μm.

Supplementary Fig. 3 BIRB 796 and SP600125 inhibited the phosphorylation (activation) of p38 MAPK and JNK, respectively, in KO cells treated with anisomycin. Confluent KO cells (clone 207-4) were cultured for 0.5 h in a high-calcium medium with a vehicle (control), 100 nM anisomycin (AM), AM plus 20 μM BIRB 796 (BIRB), or AM plus 20 μM SP600125 (SP). Total cell lysates were separated by SDS-PAGE, followed by western blotting with antibodies to phospho-p38 MAPK (P-p38), p38 MAPK (p38), phospho-JNK (P-JNK), JNK and actin. P-JNK was not detected in the control KO cells. AM increased the immunoreactivity of both P-p38 and P-JNK compared with the control. In AM-treated KO cells, BIRB 796 or SP600125 specifically inhibited the phosphorylation of p38 or JNK, respectively.

Supplementary Fig. 4 Linear localization of DSG1 to cell–cell contacts is promoted by JNK inhibition in KO cells. Confluent KO cells (clone 207-46) were cultured for 6 h in a high-calcium medium with a vehicle (a), 20 μM BIRB 796 (b), or 20 μM SP600125 (c). Cells were stained with an antibody against DSG1. In control (a),

negative, faint, or zipper-like (arrows) immunoreactivity for DSG1 was detected in cell–cell contacts. BIRB 796 treatment (b) promoted zipper-like (arrows) and linear (arrowheads) localization of DSG1 to cell–cell contacts. SP600125 treatment (c) promoted the linear (arrowheads) localization of DSG1 to cell–cell contacts. Scale bar: 10 μm.

Supplementary Fig. 5 The inhibition of JNK restores cell–cell adhesion in KO cells. Confluent WT cells were cultured for 24 h in the presence of calcium. Confluent KO cells (clone 207-46) were cultured for 24 h in the presence of calcium or calcium plus 20 μM SP600125 (SP). Cell monolayers were detached from 24-well plates by dispase, transferred to 1.5 ml tubes, vortexed, and transferred to 24-well plates. Representative images of cell monolayers subjected to dispase-based dissociation assays are shown. The number of cell monolayer fragments was counted (n = 4). Compared to the control, the number of KO cell monolayer fragments was reduced by 78.1% with SP treatment. Statistical significance was set as $*p < 0.05$, $**p < 0.01$, and $***p < 0.001$. ns: not significant.

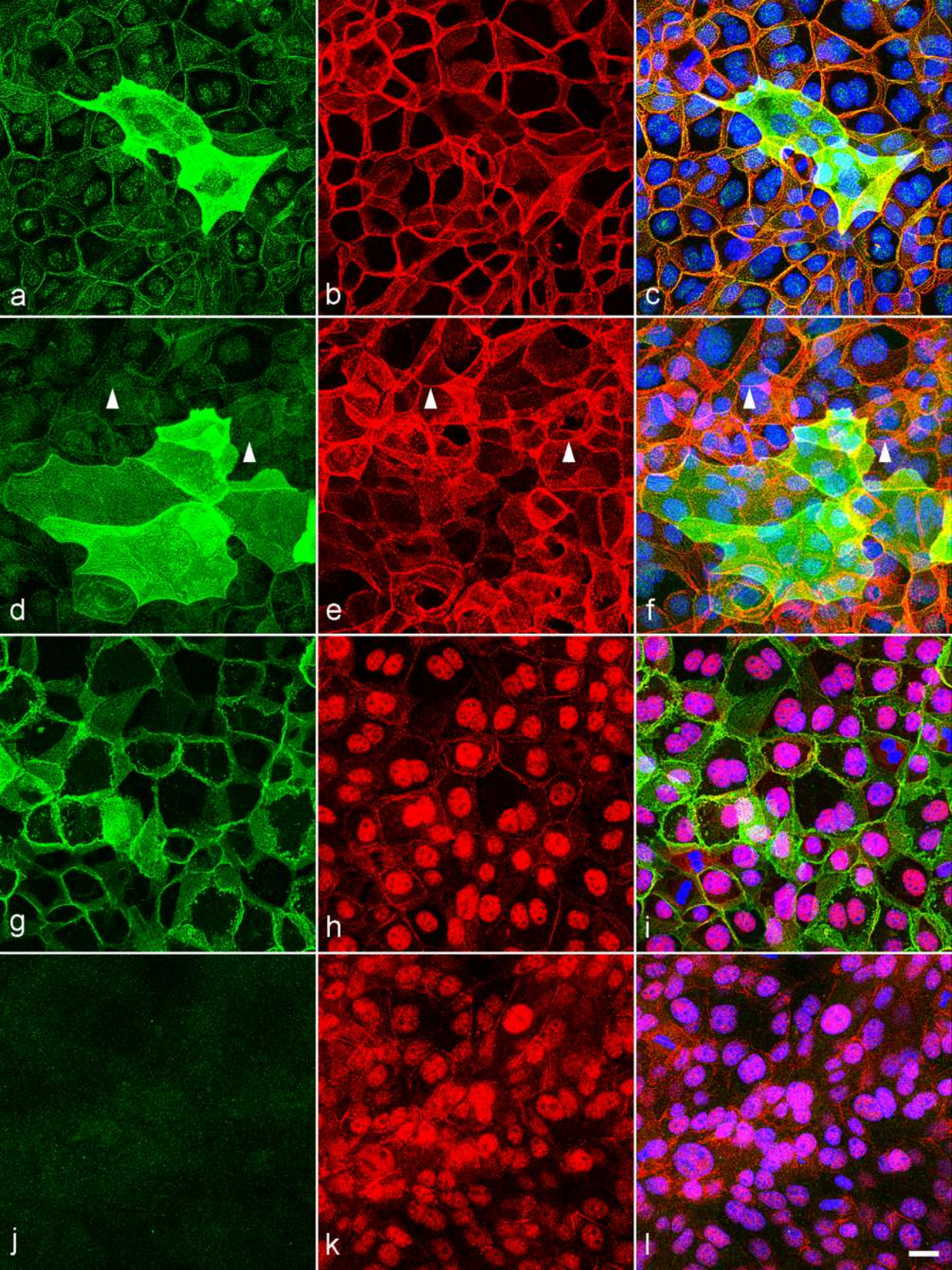
a
b
c
d
e
f
g
h
i
j
k
l

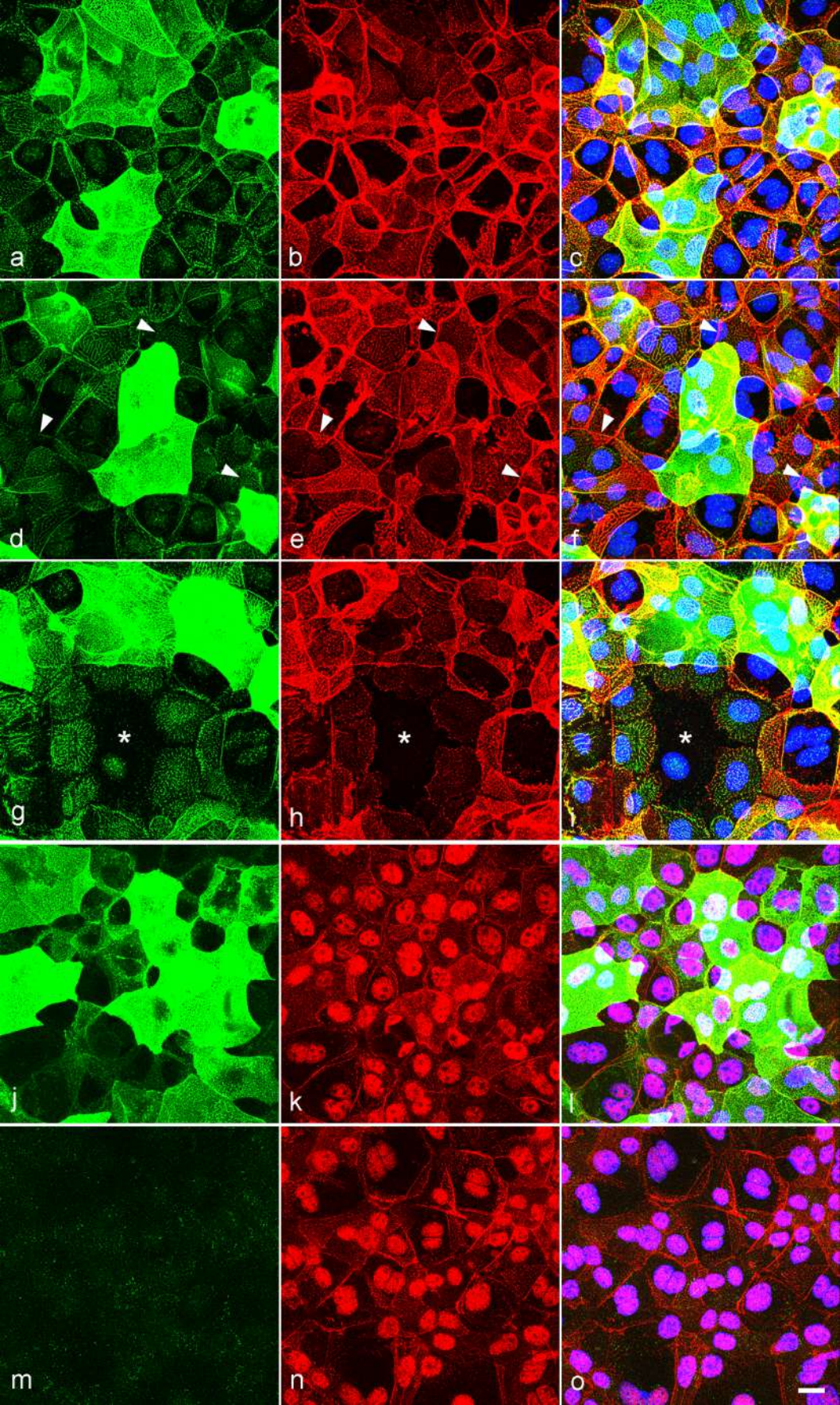
a
b
c
d
e
f
g
h
i
j
k
l
m
n
o

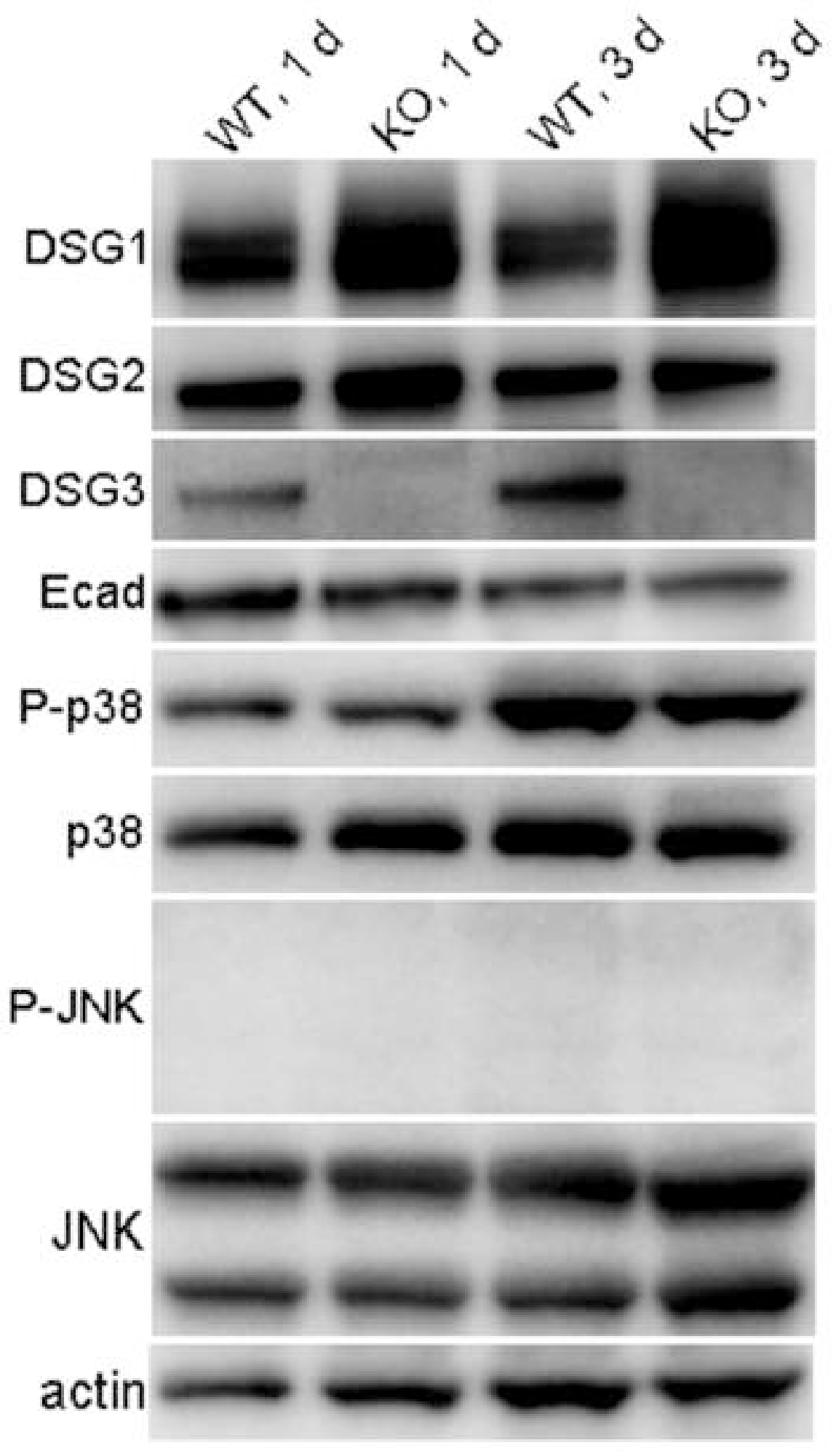
WT, 1 d
KO, 1 d
WT, 3 d
KO, 3 d
DSG1
DSG2
DSG3
Ecad
P-p38
p38
P-JNK
JNK
actin

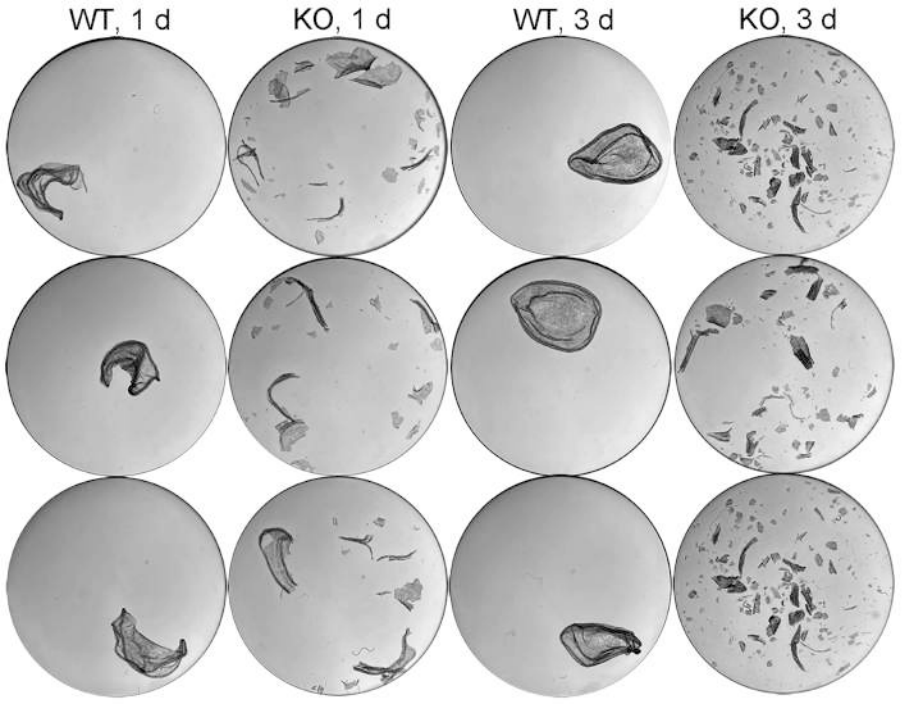
WT, 1 d
KO, 1 d
WT, 3 d
KO, 3 d

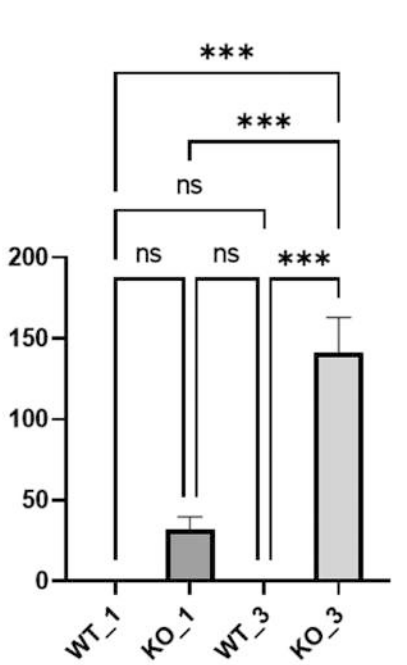
***
***
ns
ns
ns
***
200
150
100
50
0
WT_1
KO_1
WT_3
KO_3

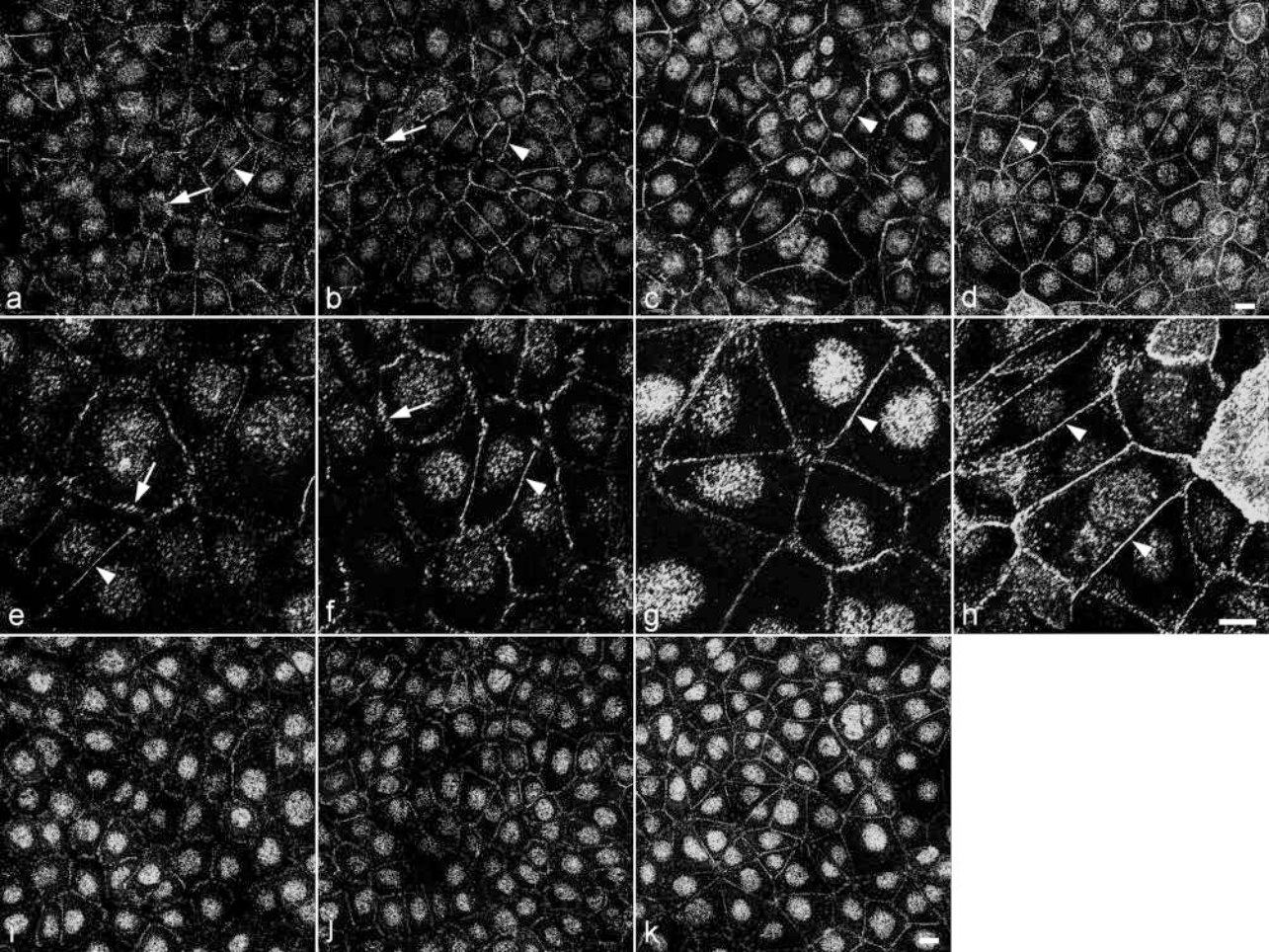
a
b
c
d
e
f
g
h
i
j
k

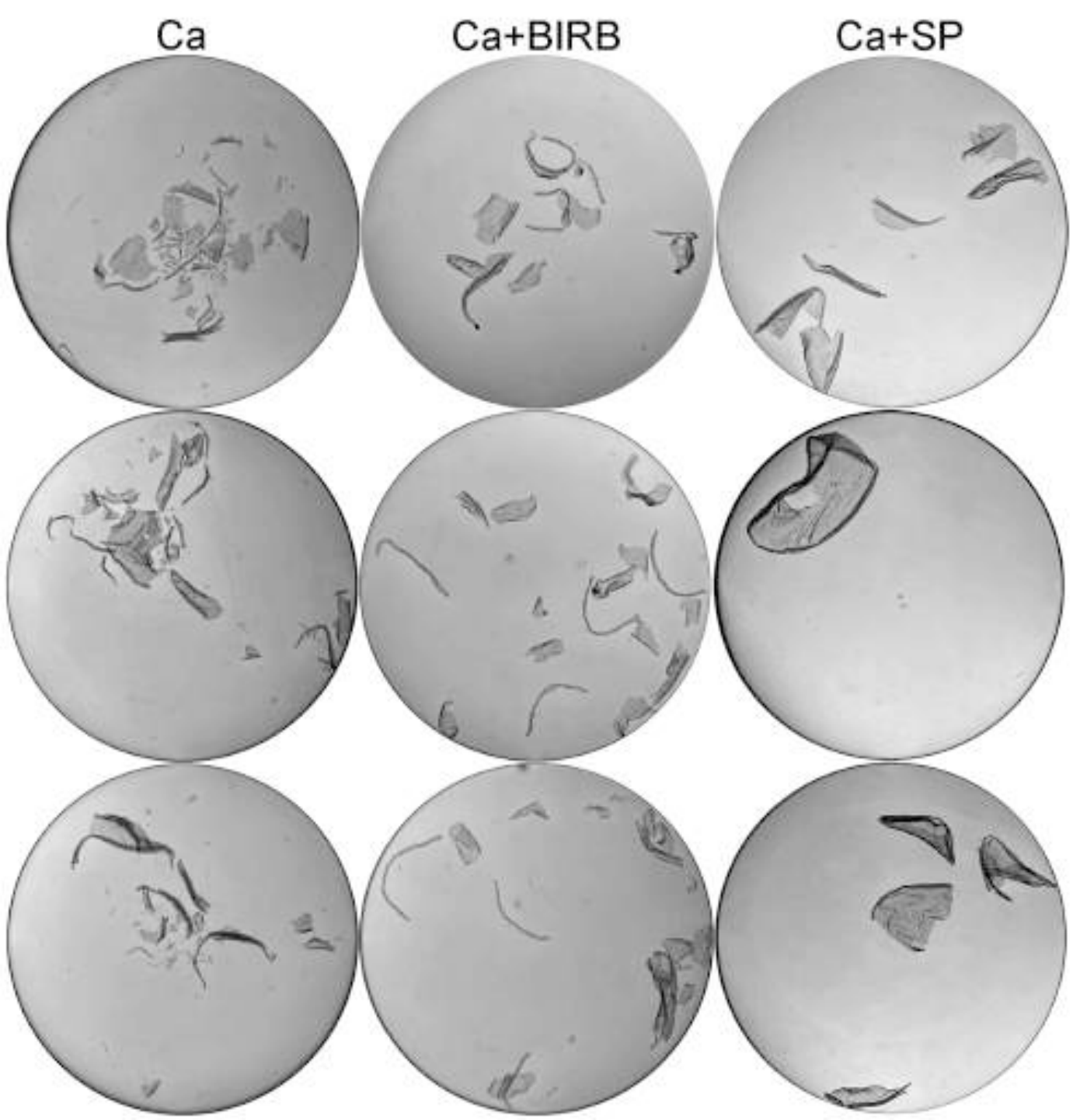
Ca
Ca+BIRB
Ca+SP

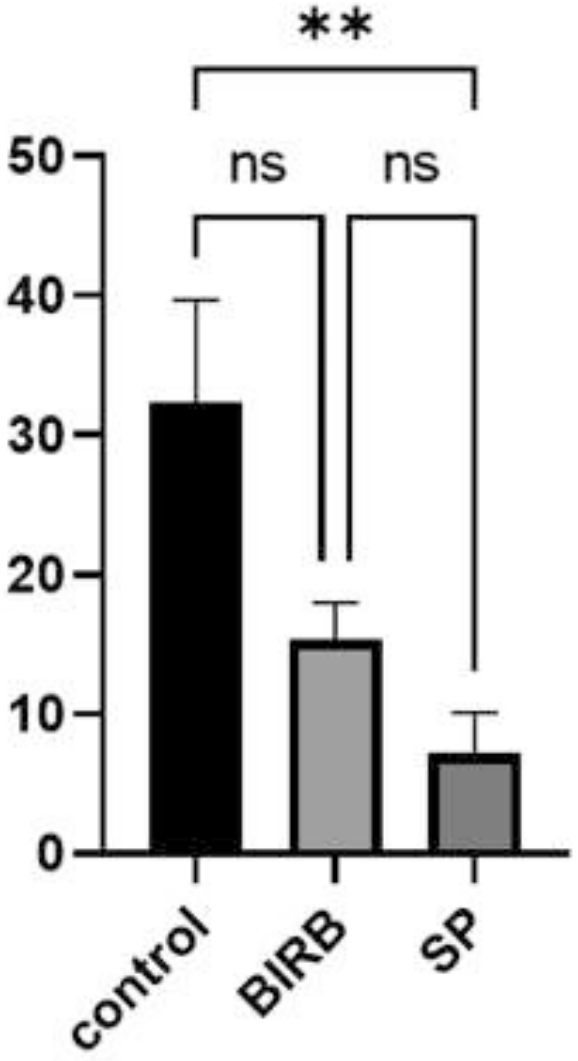
**
ns
ns
50
40
30
20
10
0
control
BIRB
SP

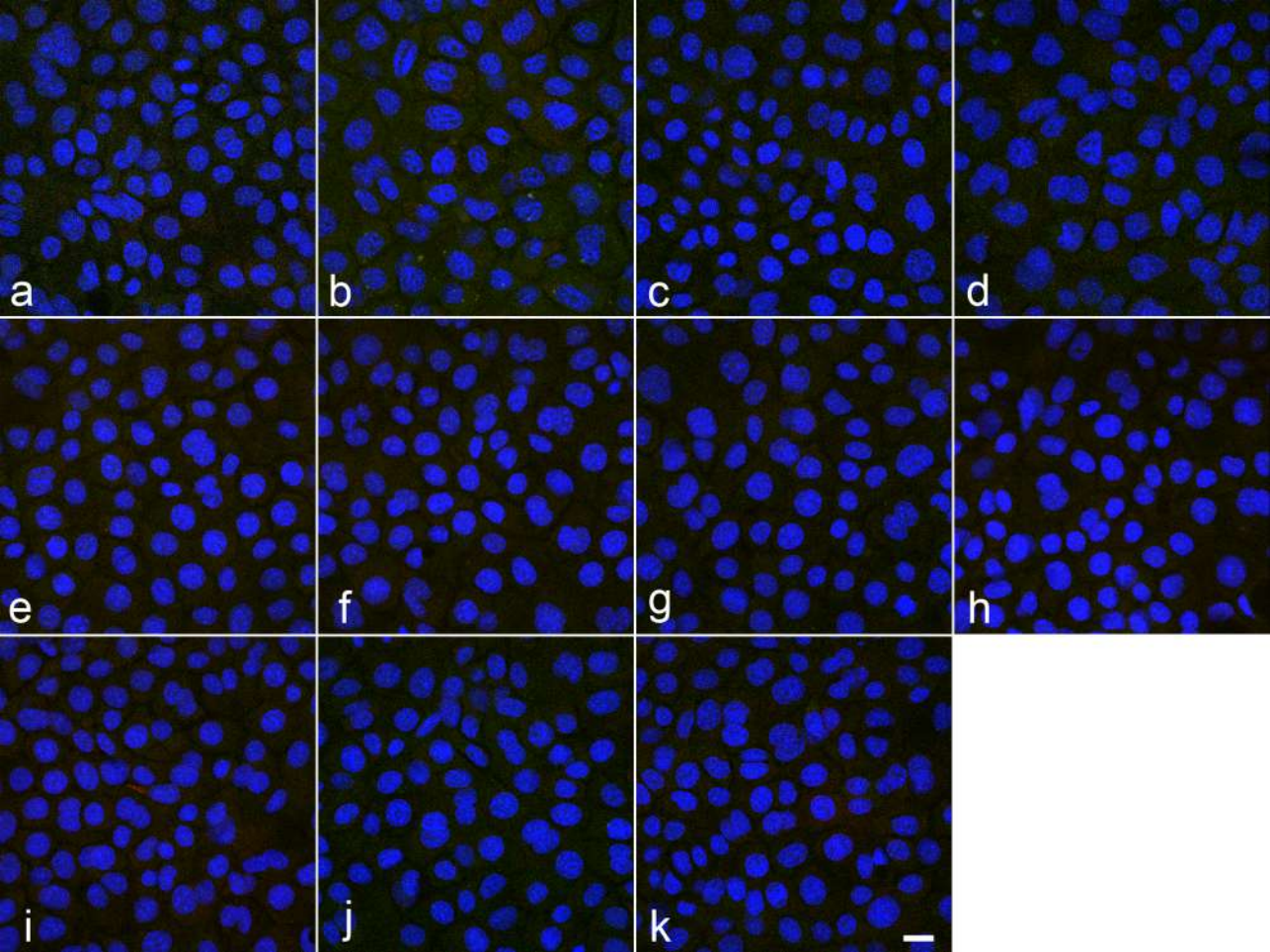
a
b
c
d
e
f
g
h
i
j
k

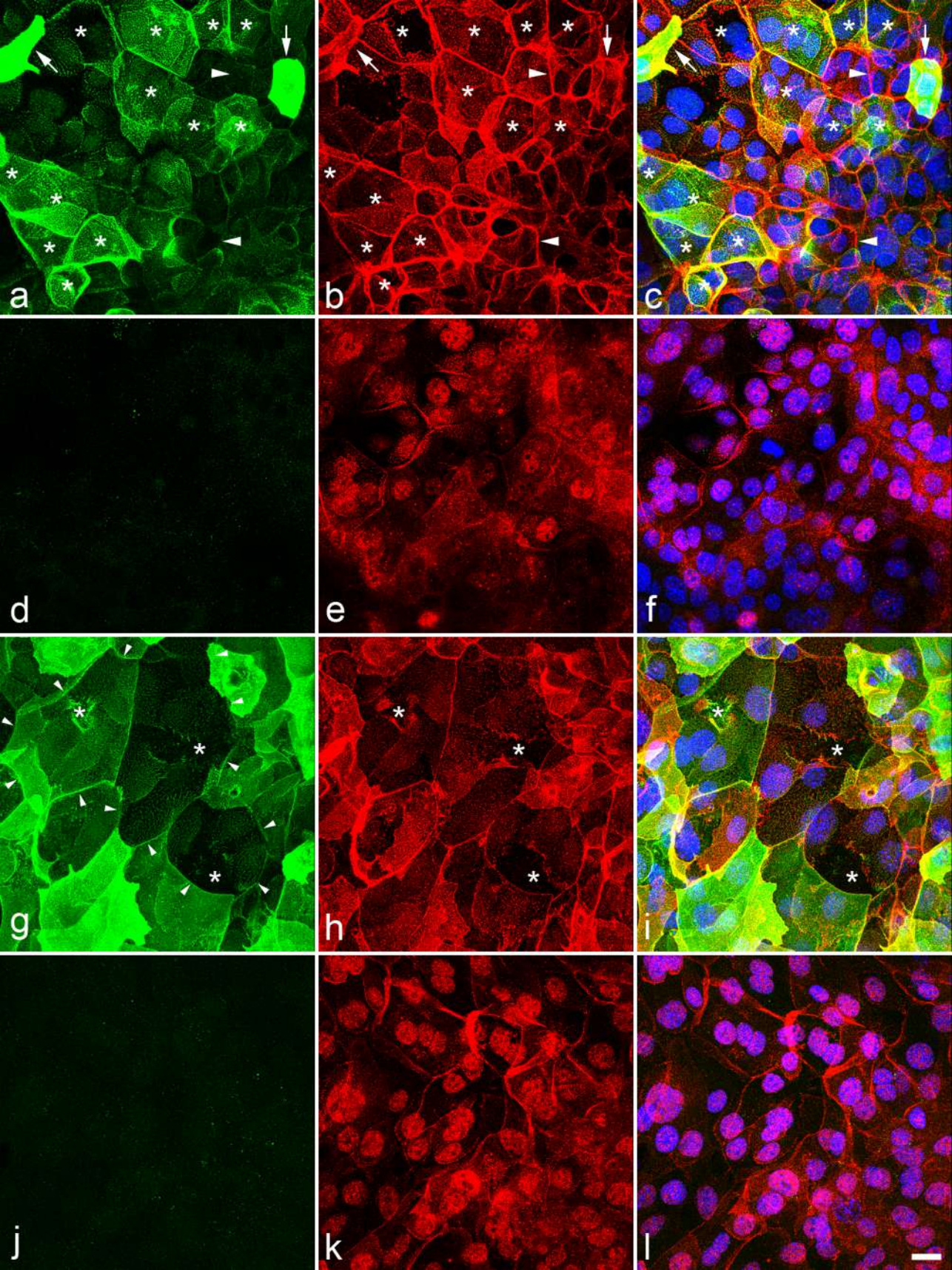
a
b
c
d
e
f
g
h
i
j
k
l

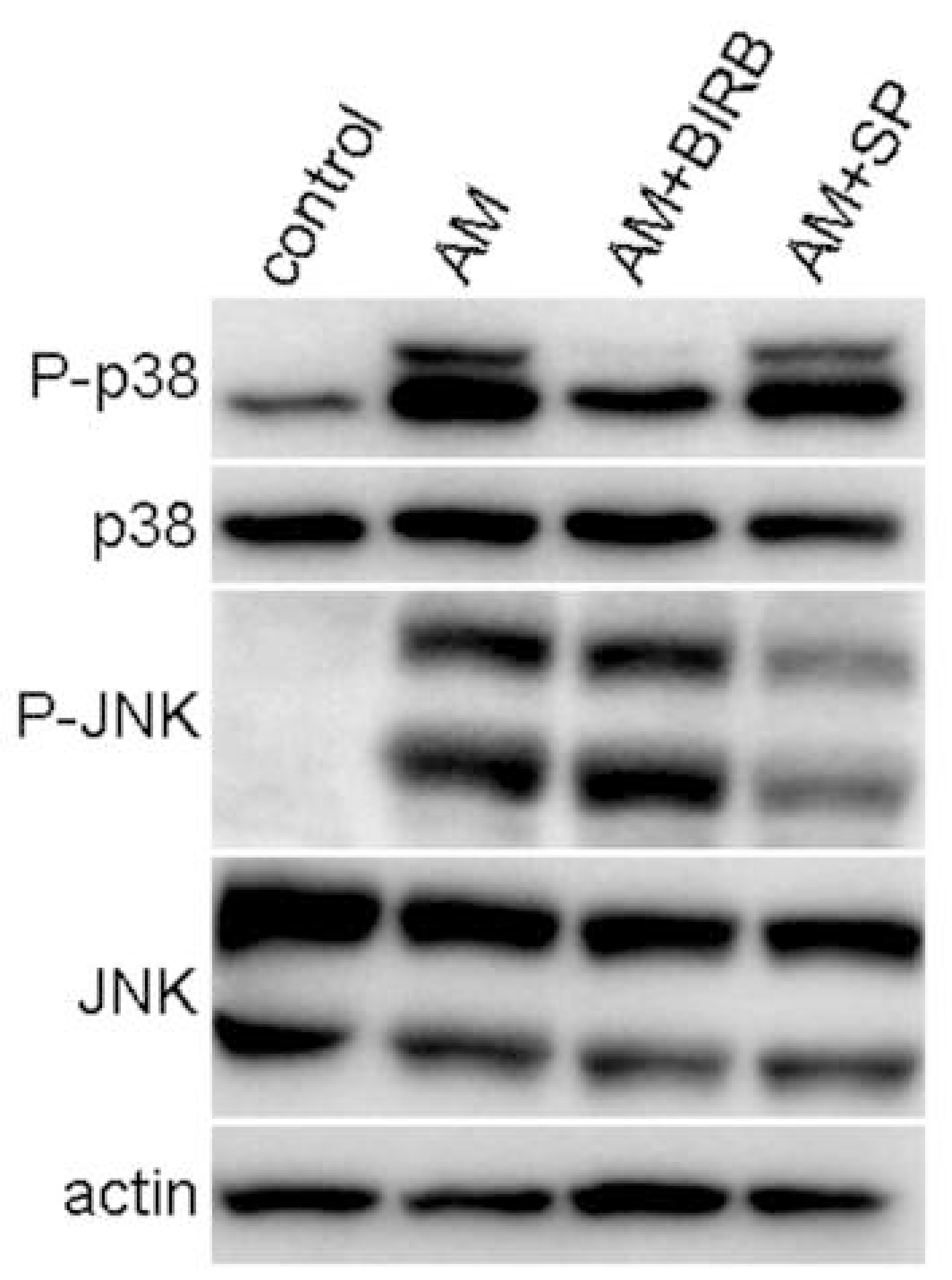
control
AM
AM+BIRB
AM+SP
P-p38
p38
P-JNK
JNK
actin

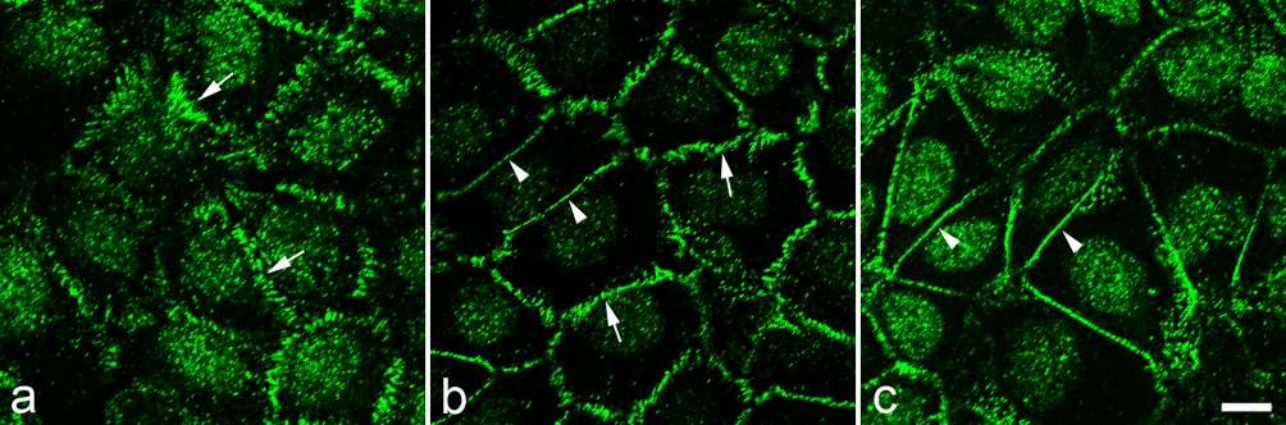
a
b
c

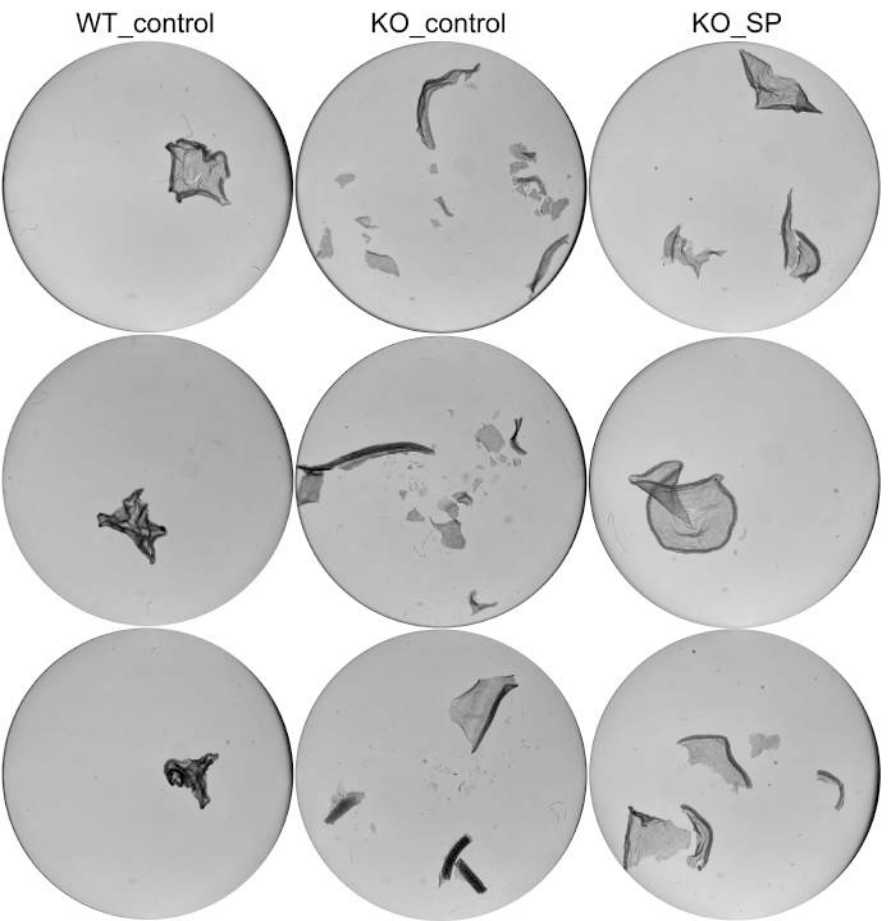
WT_control
KO_control
KO_SP

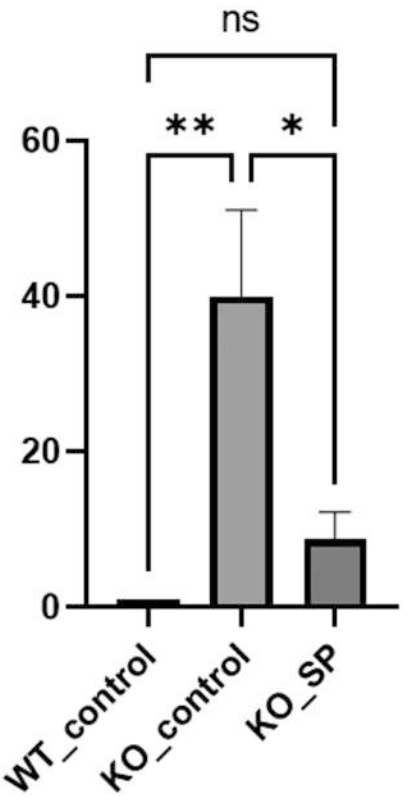
ns
**
*
60
40
20
0
WT_control
KO_control
KO_SP